6-2019

# Transient Analysis of Diffusion-Induced Deformation in a Viscoelastic Electrode

Yaohong Suo
*Fuzhou University, China*

Fuqian Yang
*University of Kentucky*, fyang2@uky.edu

**Digital Object Identifier (DOI)**
https://doi.org/10.1063/1.5052174

# Transient analysis of diffusion-induced deformation in a viscoelastic electrode

Cite as: AIP Advances **9**, 065111 (2019); https://doi.org/10.1063/1.5052174
Submitted: 14 August 2018 . Accepted: 07 June 2019 . Published Online: 18 June 2019

Yaohong Suo, and Fuqian Yang

# Transient analysis of diffusion-induced deformation in a viscoelastic electrode

Cite as: AIP Advances 9, 065111 (2019); doi: 10.1063/1.5052174
Submitted: 14 August 2018 • Accepted: 7 June 2019 •
Published Online: 18 June 2019



Yaohong Suo[1,2,a)] and Fuqian Yang[2,a)]

## AFFILIATIONS

[1]School of Mechanical Engineering and Automation, Fuzhou University, Fuzhou 350108, China
[2]Department of Chemical and Materials Engineering, University of Kentucky, Lexington, Kentucky 40506-0046, USA

[a)]Authors to whom correspondence should be addressed. E-mail address: yaohongsuo@126.com and fyang2@uky.edu.

## ABSTRACT

In this study, we analyze the transient diffuse-induced-deformation of an electrode consisting of the conducting polymer polypyrrole (PPY) by using the theories of linear viscoelasticity and diffusion-induced stress. We consider two constitutive relationships with dependence of viscosity on strain rate: Kelvin-Voigt model and three-parameter solid model. A numerical method is used to solve the problem of one-dimensional, transient diffusion-induced-deformation under potentiostatic operation. The numerical results reveal that the maximum displacement occurs at the free surface and the maximum stress occurs at the fixed end. The inertia term causes the stress to increase at the onset of lithiation. The stress decreases with increasing lithiation time and approaches zero for prolonged lithiation. Compared with the two different constitutive relationships between the Kelvin-Viogt model and three-parameter solid model, it can be found that the spatiotemporal distribution of lithium ion concentrations in the Kelvin-Viogt model is larger than that in the three-parameter solid model at the same moment, whereas the stress of the Kelvin-Viogt model is smaller owing to more than one spring in the three-parameter solid model.



## I. INTRODUCTION

Conducting polymers have attracted great interest as binders and electrode materials in lithium-ion batteries (LIBs)[1–3] and supercapacitors.[4–6] One of the challenges that currently limit the applications of conducting polymers in energy storage is the long-term volumetric swelling/shrinking during electrochemical cycling,[7–9] which can cause structural degradation and poor cycle stability.[10] It is of paramount importance to investigate cycling-induced deformation of conducting polymers and develop the constitutive relationships to describe the cycling-induced deformation.

It is known that the cycling-induced swelling/shrinking of conducting polymers is dependent on ionic transport and similar to diffusion-induced stress, which has been observed in semiconductors,[11,12] lithium-ion batteries[13,14] and sodium-ion batteries.[15,16] Most analyses of diffusion-induced stress have been based on the theories of linear elasticity,[11,12,17] large deformation,[18,19] or finite strain[20–24] with the incorporation of diffusion-induced strain or reaction-induced strain[25–27] in the corresponding constitutive relationship. However, none of these studies have addressed the diffusion-induced stress in viscoelastic materials. Recently, Yang[28] pointed out the need to carefully investigate the diffusion-induced deformation of viscoelastic materials to optimize the performance of conducting polymers in energy storage and incorporated the diffusion-induced strain in the constitutive relationship.

Considering the applications of conducting polymers in energy storage and sensing technology, we analyze the diffusion-induced stress in a viscoelastic electrode under potentiostatic operation in this study. The viscoelastic electrode is composed of polypyrrole (PPy). In contrast to the quasi-static equilibrium used in most studies, the dynamic behavior of the electrode is analyzed in this work. Both the Kelvin model and standard model are used in the analysis.

## II. MATHEMATICAL FORMULATION

### A. General formulation

Considering diffusion-induced deformation in the theory of linear viscoelasticity, the equation of motion can be expressed as

$$\sigma_{ij,i} + f_j = \rho\ddot{u}_j \quad (i,j = 1,2,3) \tag{1}$$

where $\sigma_{ij}$ are the components of the stress tensor, $f_j$ are the components of the body force, $\rho$ is density, $u_i$ is the component of the displacement vector, the comma represents the derivative with respect to spatial variables, and the dot represents the derivative with respect to time. The convention of Einstein summation for repeated indices is used in Eq. (1).

For a small deformation, the relationship between the components of strain tensor $\varepsilon_{ij}$ and the components $u_i$ of the displacement vector is

$$\varepsilon_{ij} = \frac{1}{2}(u_{i,j} + u_{j,i}) \quad (i,j = 1,2,3) \tag{2}$$

The constitutive relationship for the diffusion-induced stress in linear viscoelastic materials can be expressed as[28]

$$P\left(\sigma_{ij} - \frac{\sigma_{kk}}{3}\delta_{ij}\right) = Q\left(\varepsilon_{ij} - \frac{\varepsilon_{kk}}{3}\delta_{ij} - c\Omega\delta_{ij}\right) \tag{3}$$

where $\delta_{ij}$ is the Kronecker delta, $\Omega$ is the molar volume of solute atoms ($m^3\ mol^{-1}$), and $c$ is the concentration ($mol\ m^{-3}$) of diffusing component (solute atoms). The operators of $P$ and $Q$ are

$$P = \sum_{k=0}^{m} a_k \frac{\partial^k}{\partial t^k} \text{ and } Q = \sum_{k=0}^{n} b_k \frac{\partial^k}{\partial t^k} \tag{4}$$

where $a_k$ and $b_k$ are material constants.

According to the results reported by Yang,[12] the diffusion flux under the action of stress is

$$J_i = -D\left(c_i - \frac{\Omega c}{R\theta}\bar{\sigma}_i\right) \tag{5}$$

where $J_i$ is the component of the diffusion flux, $D$ ($m^2\ s^{-1}$) is the diffusion coefficient of the solute atoms in a stress-free solid, $R$ is the gas constant, $\theta$ is the absolute temperature, and $\bar{\sigma}$ is the hydrostatic stress. Using the mass balance, the equation for mass transport under the action of hydrostatic stress can be expressed as[12]

$$\frac{\partial c}{\partial t} = D\left(c_{ii} - \frac{\Omega c}{R\theta}\bar{\sigma}_{ii} - \frac{\Omega}{R\theta}c_i\bar{\sigma}_i\right) \tag{6}$$

## B. One-dimensional formulation

In the following analysis, we consider the problem of one-dimensional diffusion-induced deformation, as shown in Fig. 1, under potentiostatic operation. PPy, which is a viscoelastic material, is used as the electrode material. The origin of the coordinate system is on the left side of the polymer electrode, to which no traction is applied. The right side of the polymer electrode ($x = l$) is fixed and impermeable.

For the stress-free surfaces of $|y|\to\infty$ and $|z|\to\infty$, the hydrostatic stress is calculated as $\sigma/3$ where $\sigma$ is the normal stress in the $x$ direction. The motion equation without the body force, the diffusion equation and the diffusive flux are simplified as

$$\frac{\partial \sigma}{\partial x} = \rho\ddot{u} \tag{7}$$

$$\frac{\partial c}{\partial t} = D\frac{\partial}{\partial x}\left(\frac{\partial c}{\partial x} - \frac{\Omega c}{3R\theta}\frac{\partial \sigma}{\partial x}\right) \tag{8}$$

$$J = -D\left(\frac{\partial c}{\partial x} - \frac{\Omega c}{3R\theta}\frac{\partial \sigma}{\partial x}\right) \tag{9}$$

For the Kelvin–Voigt model, Eq. (4) gives

$$\sigma(x,t) = E[\varepsilon(x,t) - \frac{1}{3}c(x,t)\Omega] + \eta[\dot{\varepsilon}(x,t) - \frac{1}{3}\dot{c}(x,t)\Omega] \tag{10}$$

where $\varepsilon(x, t)$ is uniaxial strain, $E$ is the elastic modulus and $\eta$ is the viscosity. For the three-parameter solid model in Fig. 2, Eq. (4) gives

$$\sigma + \frac{\eta}{E_1 + E_2}\dot{\sigma} = \frac{E_1E_2}{E_1 + E_2}[\varepsilon(x,t) - \frac{1}{3}c(x,t)\Omega] + \frac{\eta E_2}{E_1 + E_2}[\dot{\varepsilon}(x,t) - \frac{1}{3}\dot{c}(x,t)\Omega] \tag{11}$$

where $E_1$ and $E_2$ are elastic moduli. Comparing with Eqs. (10) and (11), it can be seen that the three-parameter solid model will reduce to the Kelvin-Voigt model when $E_1 >> E_2$.

PPy is a non-Newtonian polymer. When $c = 0$, $\eta$ of PPy at 25 °C as a function of strain is[16]

$$\eta = 14.05 - 8.4 \times 10^{-3}\dot{\varepsilon}(x,t) + 2.79 \times 10^{-6}\dot{\varepsilon}^2(x,t) \tag{12}$$

Considering the effect of the diffusion-induced strain on $\eta$, Eq. (12) can be modified as

$$\eta = 14.05 - 8.4 \times 10^{-3}[\dot{\varepsilon}(x,t) - \frac{1}{3}\dot{c}(x,t)\Omega] + 2.79 \times 10^{-6}[\dot{\varepsilon}(x,t) - \frac{1}{3}\dot{c}(x,t)\Omega]^2 \tag{13}$$

which indicates that the diffusion/migration of solute atoms in PPy can cause a change of the local viscosity during viscoelastic deformation.

The initial conditions are

$$u(x,0) = 0,\ \sigma(x,0) = 0,\ \text{and } c(x,0) = 0 \tag{14}$$

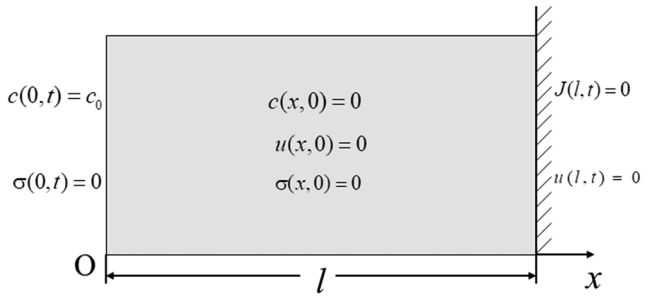


**FIG. 1**. Schematic of one-dimensional problem.

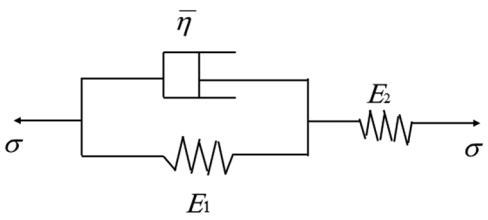


**FIG. 2**. Schematic of a three-parameter solid model.

The boundary conditions of the deformation are

$$u(l,t) = 0 \text{ and } \sigma(0,t) = 0 \tag{15}$$

and the boundary conditions of the diffusion under potentiostatic operation are

$$c(0,t) = c_0 \text{ and } J(l,t) = 0 \tag{16}$$

By introducing the following dimensionless variables,

$$C = \frac{c}{c_0},\ X = \frac{x}{l},\ T = \frac{Dt}{l^2},\ U = \frac{u}{l},\ \tilde{\sigma} = \frac{\sigma}{E},\ \text{and } \tilde{\eta} = \frac{\eta}{E}\cdot\frac{D}{l^2} \tag{17}$$

Eq. (7) and (8) can be written as

$$\frac{\partial C}{\partial T} = \frac{\partial}{\partial X}\left(\frac{\partial C}{\partial X} - qC\frac{\partial \tilde{\sigma}}{\partial X}\right) \quad \text{for } 0 \le X \le 1 \tag{18}$$

$$b\cdot\frac{\partial^2 U}{\partial T^2} - \frac{\partial \tilde{\sigma}}{\partial X} = 0 \quad \text{for } 0 \le X \le 1 \tag{19}$$

The constitutive relationships in Eq. (10) and (11) in dimensionless form are

$$\tilde{\sigma} = \frac{\partial U}{\partial X} - n\cdot C + \tilde{\eta}\left(\frac{\partial^2 U}{\partial X \partial T} - n\frac{\partial C}{\partial T}\right) \tag{20}$$

for the Kelvin–Voigt model, and

$$\tilde{\sigma} + \frac{\tilde{\eta}}{2}\frac{d\tilde{\sigma}}{dT} = \frac{1}{2}\left(\frac{\partial U}{\partial X} - n\cdot C\right) + \frac{\tilde{\eta}}{2}\left(\frac{\partial^2 U}{\partial X \partial T} - n\frac{\partial C}{\partial T}\right) \tag{21}$$

for the three-parameter solid model with $E_1 = E_2 = E$. Here, the parameters $q$, $n$, and $b$ are calculated as

$$q = \frac{\Omega E}{3R\theta},\ n = \frac{\Omega c_0}{3},\ \text{and } b = \frac{\rho D^2}{El^2} \tag{22}$$

The corresponding boundary conditions in dimensionless form are

$$C(0,T) = 1,\ J(T,1) = 0,\ \tilde{\sigma}(0,T) = 0,\ \text{and } U(1,T) = 0 \tag{23}$$

and the corresponding initial conditions in dimensionless form are

$$C(X,0) = 0,\ U(X,0) = 0,\ \text{and } \tilde{\sigma}(X,0) = 0 \tag{24}$$

## III. RESULTS OF NUMERICAL SIMULATIONS AND DISCUSSION

Both the Kelvin-Voigt and three-parameter solid models are used to describe the viscoelastic behavior of PPy in the numerical analysis of the diffusion-induced deformation of a PPy electrode during electrochemical lithiation. The material properties used in the numerical calculation of the lithiation of PPy are $D = 2.78 \times 10^{-15}$ $m^2 \cdot s^{-1}$,[29] $E$ =100 MPa,[29] $\Omega$ =1.86 × $10^{-6}$ $m^3 \cdot mol^{-1}$,[30] $l = 3 \times 10^{-7}$ m, R = 8.314 $J \cdot K^{-1} mol^{-1}$, and θ = 298 K.

### A. Kelvin-Voigt model of PPy

Figure 3a shows the spatial distribution of lithium in the PPy electrode at different lithiation times. The Li-concentration decreases with the decrease of the distance to the fixed surface at the same diffusion time, and the concentration gradually increases with the increase of the lithiation time. When the lithiation time approaches infinity, the concentration of lithium in the PPy electrode becomes uniform, as expected.

Figure 3b depicts the spatial distributions of the displacement in the PPy electrode at different lithiation times. The PPy undergoes expansion with the traction-free surface moving in the direction opposite to the $x$ direction. The traction-free surface has the maximum displacement magnitude. When the lithiation time approaches infinity, the displacement becomes a linear function of the spatial variables.

The spatial distributions of the strain in the PPy electrode at different lithiation times are depicted in Fig. 3c. At the same lithiation time, the strain decreases with decreasing distance to the fixed surface owing to the displacement constraint, as shown in Fig. 3b. At a fixed spatial position, the strain increases with lengthening lithiation time because of the continuous diffusion/migration of lithium into the PPy electrode and the diffusion-induced strain. The difference in the strain at two different spatial positions decreases with extending of the lithiation time, and the strain in the PPy electrode becomes independent of the spatial variables when the lithiation time approaches infinity, in agreement with the spatial distributions of the displacement provided in Fig. 3b.

Figure 3d depicts the spatial distributions of the stress in the PPy electrode at different lithiation times. The stress increases with the decrease of the distance to the fixed surface at the same lithiation time, and the stress gradually decreases with the increase of the lithiation time. When the diffusion time approaches infinity, the stress in the PPy electrode becomes zero, as expected.

The temporal evolution of the stress at several positions of the PPy electrode is presented in Fig. 3e. The stress at each spatial position initially increases from zero to a finite value very quickly and then gradually decreases to zero for prolonged lithiation. Note that the temporal evolution of the stress is mainly caused by the inertial term in the equation of motion Eq. (1) or (7). If the contribution of the inertial term in Eq. (1) or (7) is negligible, i.e., the characteristic time for the mechanical deformation of the PPy electrode is much shorter than the characteristic time for the diffusion/migration of lithium in the PPy electrode, the one-dimensional equilibrium equation (7) can be written as

$$\frac{\partial \sigma}{\partial x} = 0 \tag{25}$$

which together with the boundary condition $\sigma(0, t) = 0$ gives $\sigma(x, t) = 0$ in the PPy electrode during the lithiation. It is the inertial term in the equation of motion that leads to the temporal evolution of the stress in the PPy electrode and the temporal evolution of the stress is similar to that of Ref. 31.

### B. Three-parameter solid model of PPy

Here, we assume that the viscoelastic behavior of the PPy electrode during lithiation can be described by the three-parameter solid model shown in Fig. 2 with $E_1 = E_2 = E$ in the numerical analysis. Figure 4a depicts the spatial distributions of lithium in the PPY electrode at different diffusion times. Similar to the results obtained from the Kelvin-Voigt model, the Li concentration decreases with the decrease of the distance to the fixed surface at the same lithiation time, and the concentration gradually increases with the increase of the lithiation time. The difference in the lithium concentration

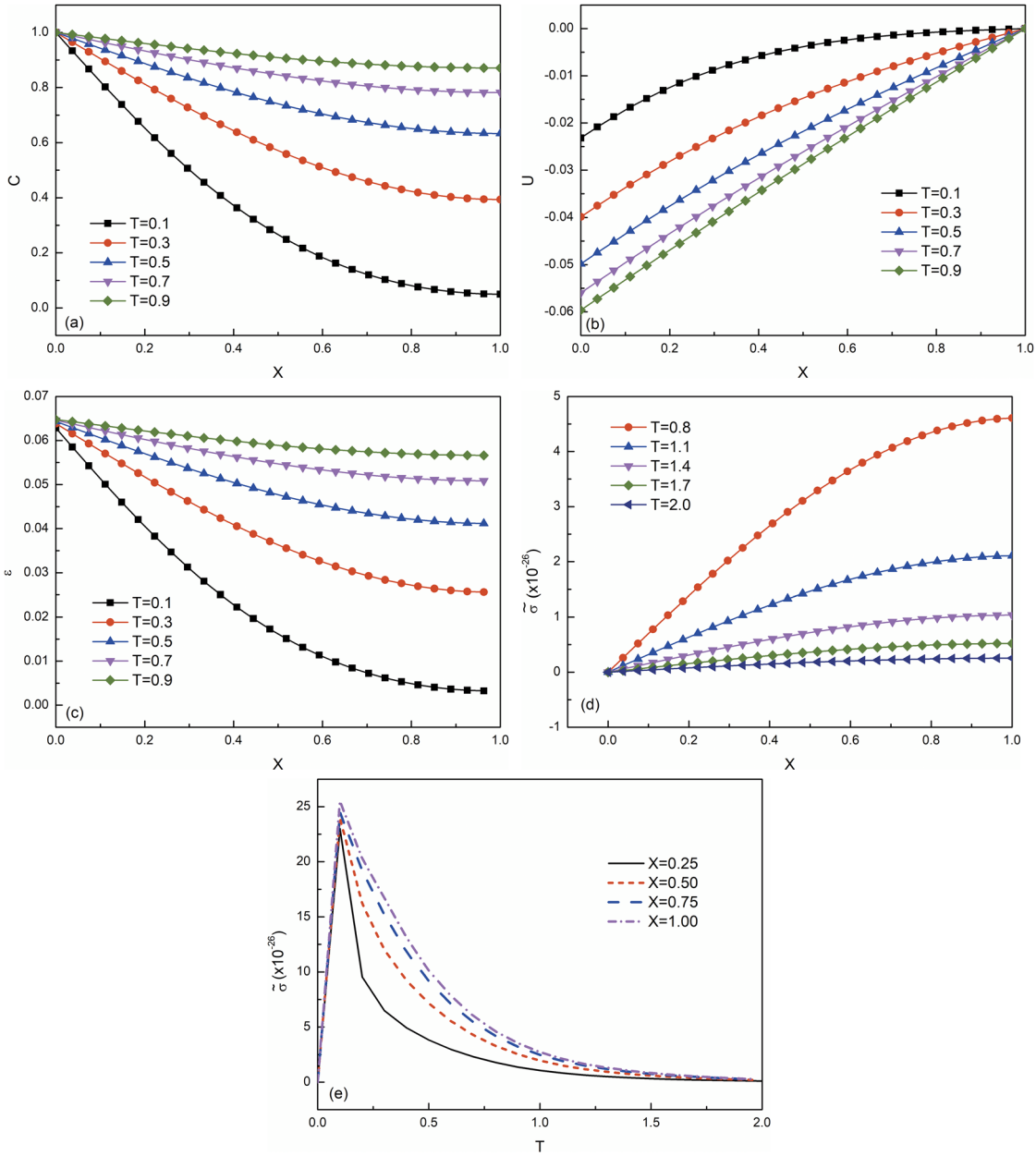


**FIG. 3**. Spatial distributions of (a) Li concentration, (b) displacement, (c) strain, (d) stress at different lithiation times, and (e) temporal distribution of stress at different positions in the Kelvin-Voigt model.

between two different positions decreases with lengthening the lithiation time. When the lithiation time approaches infinity, the concentration of lithium in the PPy electrode becomes uniform, as expected.

Figure 4b shows the spatial distributions of the displacement in the PPY electrode at different lithiation times. The PPy experiences expansion because of the diffusion-induced volumetric change, and the traction-free surface moves in the opposite $x$-direction. The traction-free surface has the maximum displacement magnitude, which is similar to the results obtained from the Kelvin-Voigt model. When the lithiation time approaches infinity, the displacement becomes a linear function of the spatial variables.

The spatial distributions of the strain in the PPy electrode at different lithiation times are depicted in Fig. 4c. At the same lithiation time, the strain decreases with decreasing the distance to the fixed surface, similar to the results obtained from the Kelvin-Voigt

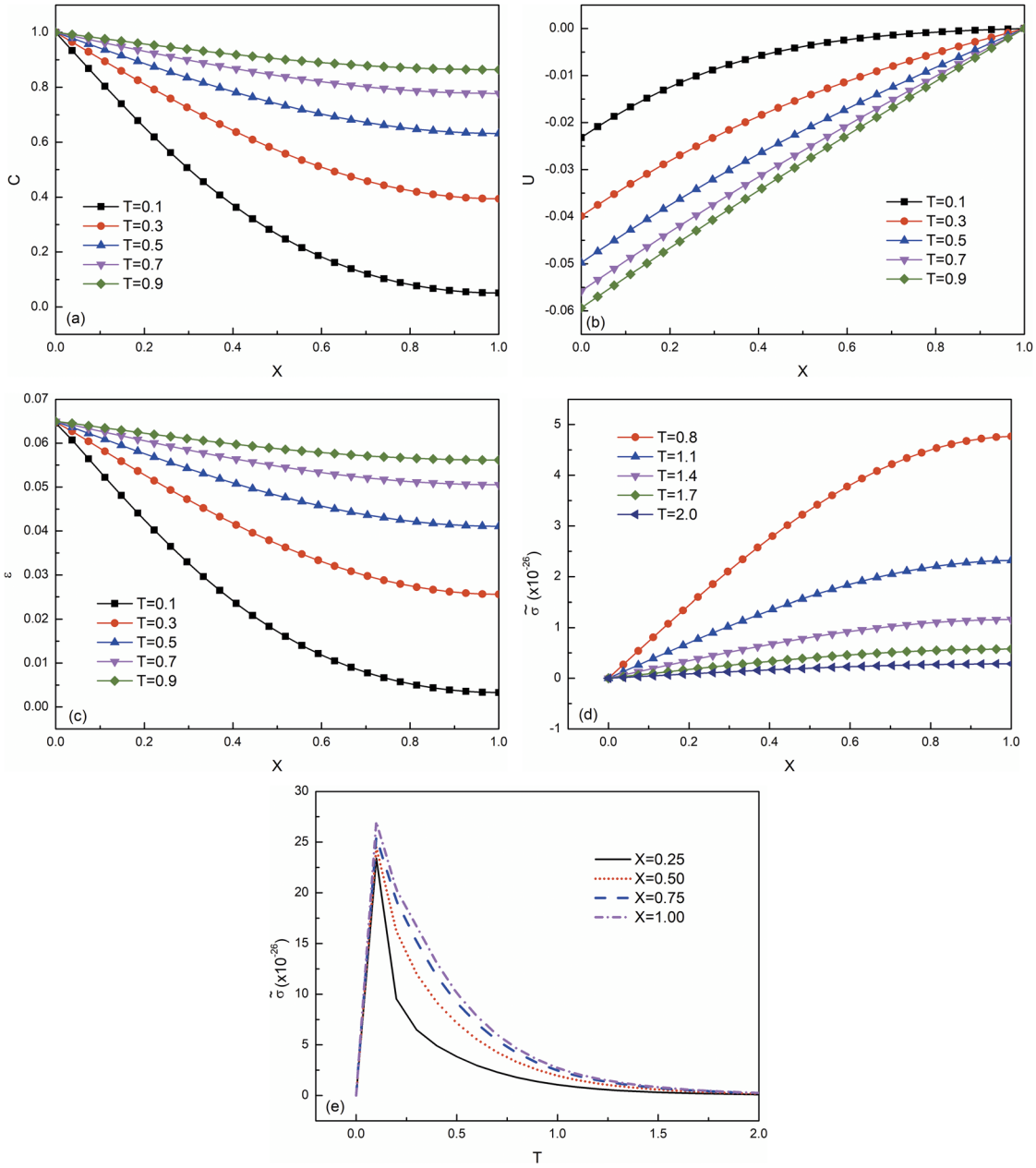


**FIG. 4**. Spatial distribution of (a) Li concentration, (b) displacement, (c) strain, (d) stress at different lithiation times, and (e) temporal distribution of stress at different positions in three-parameter solid model.

model. At a fixed spatial position, the strain increases with increasing the lithiation time. Such a result is controlled by the diffusion/migration of lithium into the PPy electrode and the diffusion-induced strain. Similar to the results obtained from the Kelvin-Voigt model, the difference in the strain at two different spatial positions decreases with lengthening lithiation time. In addition, the strain in the PPy electrode becomes independent of the spatial variables when the lithiation time approaches infinity, in agreement with the spatial distribution of the displacement presented in Fig. 4b.

The spatial distributions of the stress at different lithiation times in the PPy electrode are depicted in Fig. 4d. At the same lithiation time, the stress decreases with the increase of the distance to the fixed end, similar to the results from the Kelvin-Voigt model.

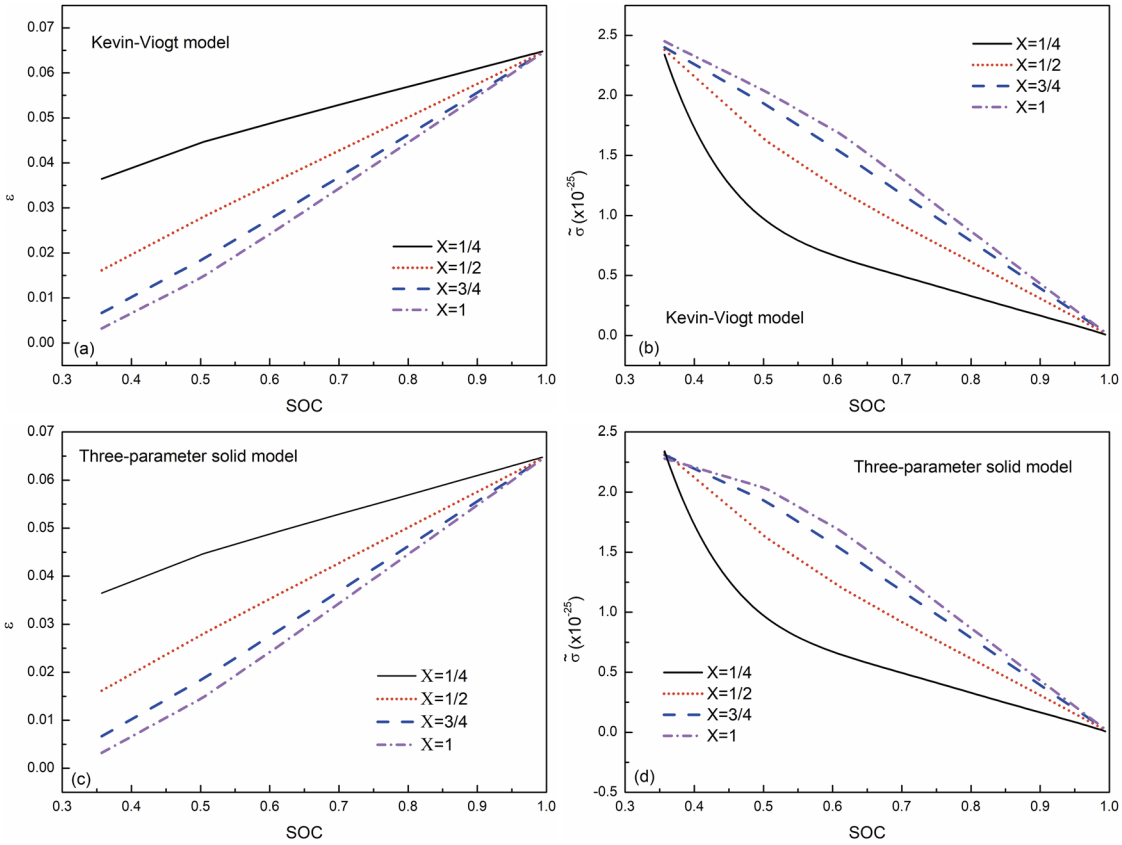


**FIG. 5**. (a) Variation of the strain with SOC at X = ¼, ½ , ¾, and 1 for the Kevin-Voigt model, (b) variation of the stress with SOC at X = ¼, ½, ¾, and 1 for the Kevin-Voigt model, (c) variation of the strain with SOC at X = ¼, ½, ¾, and 1 for the three-parameter solid model, (d) variation of the stress with SOC at X = ¼, ½, ¾, and 1 for the three-parameter solid model.

The largest stress occurs at the fixed end. Extending the lithiation time leads to a decrease of the stress.

The temporal evolution of the stress at several positions (X = 1/4, 1/2, 3/4, and 1) of the PPy electrode is shown in Fig. 4e. Similar to the results from the Kelvin-Voigt model, the stress at each spatial position initially increases from zero to a finite value very quickly, and then gradually decreases to zero after prolonged lithiation. The inertial term in the equation of motion Eq. (1) or (7) mainly causes the stress to rise abruptly from the initial stress value (0). With the increasing of the diffusion time, diffusion will approach to the steady and the lithium ion concentration will be uniform distribution, which means that the stress will finally become a constant, and this constant should be zero by combining the boundary condition (Eq. (15)). Therefore, the stress will gradually decrease for the longer diffusion time and finally will approach zero at the fully lithiatied state.

The state of charge (SOC), an important parameter for the energy storage, is expressed as

$$SOC = \frac{\int_0^l c(x,t)dx}{\int_0^l c_0 dx} = \int_0^1 C(X,T)dX \tag{26}$$

The variations of the strain and stress with SOC at $X$ = ¼, ½, ¾, and 1 for both the Kevin-Voigt model and three-parameter solid model are presented in Fig. 5. The strain increases with rising SOC for both models, consistent with the temporal evolution of the strain shown in Fig. 3 and 4. The stress decreases with increasing SOC for both models because larger concentration leads to larger SOC for longer time and smaller stresses occurs with larger diffusion time which can be seen from Figs. 3(d) and 4(d). There exist the similar trends and fewer differences in the spatiotemporal distribution of lithium and stress in the PPy electrode for these two constitutive relationships.

## C. Comparisons

The comparisons of the concentration between the Kelvin model and three-parameter solid model are exhibited in Fig. 6a at different times. It can be seen that the concentrations in Kelvin model are larger than those in the three-parameter solid model at the same moment. This phenomenon is due to that the number of the springs in the three-parameter solid model is 1 more than that in Kelvin model, and this spring prevents more lithium ions into PPY electrode, and then leads to smaller concentration in the

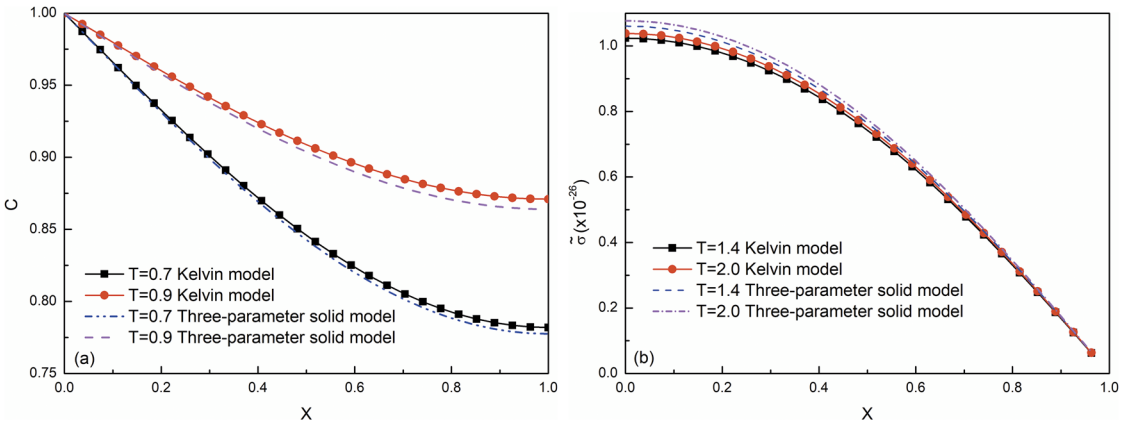


**FIG. 6**. Comparision of the concentration (a) and stress (b) between the Kelvin model and Three-parameter solid model.

three-parameter solid model at the same time and the same position. Fig. 6b shows the comparisons of the stress in Kelvin model and in three-parameter model at different times. The stress in the three-parameter model is larger than that in the Kelvin model. The spring in the three-parameter solid model enlarges the deformation and results in larger stress.

The comparisons of the Li ions concentration among pure diffusion, the Kelvin model and three-parameter solid model are made in Fig. 7. It can be seen that the concentration in the Kelvin and three-parameter model is larger than that in pure diffusion at the same position and same time. Such results are due to stress-induced diffusion in the Kelvin and three-parameter model. However, the concentration in the three-parameter model is smaller than that of the Kelvin model because the spring prevents more lithium ions into PPY electrode in the three-parameter model.

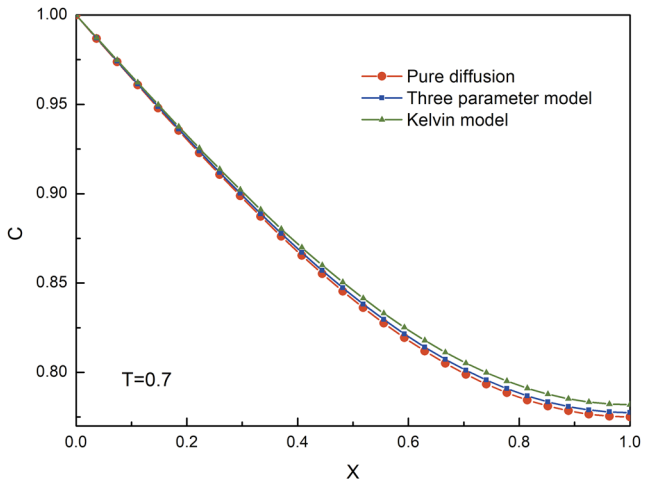


**FIG. 7**. Comparison of the concentration among pure diffusion, the Kelvin model and Three-parameter solid model.

## IV. SUMMARY

In this work, we have analyzed the transient, viscoelastic deformation of a one-dimensional PPy electrode induced by the diffusion of lithium under potentiostatic operation. The Kelvin and three-parameter solid model are used as two different viscoelastic models with the viscosity in which the viscosity is considered as a function of the strain rate. The numerical results reveal the important role of the inertial term in controlling the stress evolution in the electrode. At the onset of potentiostatic operation, the stress increased rapidly in the electrode, with the largest stress at the fixed end. The stress in the electrode decreases with lengthening lithiation time and approaches zero after prolonged lithiation. The electrode experiences expansion towards the traction-free surface. The largest displacement occurs at the traction-free end regardless of the constitutive relationships used, and the displacement becomes a linear function of the spatial variable after prolonged lithiation. Finally, the spatiotemporal distributions of lithium ion concentration and stress in the electrode are compared between Kelvin model and the three parameter model. The simulated results show that the lithium ion concentration in Kelvin-Viogt model is larger than that in the three-parameter solid model at the same moment, whereas the stress of Kelvin-Viogt model is smaller. This phenomenon is due to that more than one spring in the three-parameter solid prevents more lithium ions into PPY electrode, and enlarges the deformation and results in larger stress.

Currently, there are no experimental results of lithium-induced deformation of polymer electrode materials available in literature, since most works have been focused on advanced materials, including Sn and Sb, in improving the energy storage of lithium-ion batteries, and it is very difficult to in-situ measure the deformation of active materials used in lithium-ion batteries. To validate the analyses presented in this work, experimental work similar to lithium-induced expansion of Si-islands should be designed and performed. The temporal change in the geometrical dimensions of polymer islands during charging and discharging needs to be measured to reveal the effect of lithiation and de-lithiation on the viscoelastic deformation of polymer.

## ACKNOWLEDGMENTS

Y.S. is grateful for the support by NSFC (Grant No. 11402054), Natural Science Foundation of Fujian Provincial (Grant No. 2018J01663) and Scientific Research Program Funded by Fujian Provincial Education Commission (Grant No. JT180026). F.Y. is grateful for the support by the NSF through the grant CMMI-1634540, monitored by Dr. Khershed Cooper. We thank Liwen Bianji for editing the English.

## REFERENCES

[1]R. Rohan *et al.*, "Functionalized polystyrene based single ion conducting gel polymer electrolyte for lithium batteries," Solid State Ionics **268**, 294–299 (2014).
[2]H. Y. Yan, G. Zhang, and Y. F. Li, "Synthesis and characterization of advanced $Li_3V_2(PO_4)_3$ nanocrystals@conducting polymer PEDOT for high energy lithium-ion batteries," Applied Surface Science **393**, 30–36 (2017).
[3]F. Wu *et al.*, "Surface modification of Li-rich cathode materials for lithium-ion batteries with a PEDOT:PSS conducting polymer," ACS Applied Materials & Interfaces **8**(35), 23095–23104 (2016).
[4]K. Lepicka *et al.*, "A redox conducting polymer of a meso-Ni(II)-SaldMe monomer and its application for a multi-composite supercapacitor," Electrochimica Acta **268**, 111–120 (2018).
[5]Q. F. Meng *et al.*, "Research progress on conducting polymer based supercapacitor electrode materials," Nano Energy **36**, 268–285 (2017).
[6]D. D. Potphode *et al.*, "Asymmetric supercapacitor devices based on dendritic conducting polymer and activated carbon," Electrochimica Acta **230**, 29–38 (2017).
[7]Y. Huang *et al.*, "Nanostructured polypyrrole as a flexible electrode material of supercapacitor," Nano Energy **22**, 422–438 (2016).
[8]A. Afzal *et al.*, "Polypyrrole/carbon nanotube supercapacitors: Technological advances and challenges," Journal of Power Sources **352**, 174–186 (2017).
[9]P. M. Dziewonski and M. Grzeszczuk, "Impact of the electrochemical porosity and chemical composition on the lithium ion exchange behavior of polypyrroles ($ClO_4^-$, $TOS^-$, $TFSI^-$) prepared electrochemically in propylene carbonate. Comparative EQCM, EIS and CV studies," Journal of Physical Chemistry B **114**(21), 7158–7171 (2010).
[10]Q. H. Yu *et al.*, "Construction of tubular polypyrrole-wrapped biomass-derived carbon nanospheres as cathode materials for lithium-sulfur batteries," Journal of Physics D-Applied Physics **50**(11), 115002 (2017).
[11]S. Prussin, "Generation and distribution of dislocations by solute diffusion," Journal of Applied Physics **32**(10), 1876–1881 (1961).
[12]F. Q. Yang, "Interaction between diffusion and chemical stresses," Materials Science and Engineering A-Structural Materials Properties Microstructure and Processing **409**(1-2), 153–159 (2005).
[13]M. N. Obrovac and L. Christensen, "Structural changes in silicon anodes during lithium insertion/extraction," Electrochemical and Solid State Letters **7**(5), A93–A96 (2004).
[14]E. M. C. Jones *et al.*, "Reversible and irreversible deformation mechanisms of composite graphite electrodes in lithium-ion batteries," Journal of the Electrochemical Society **163**(9), A1965–A1974 (2016).
[15]Y. You *et al.*, "A zero-strain insertion cathode material of nickel ferricyanide for sodium-ion batteries," Journal of Materials Chemistry A **1**(45), 14061–14065 (2013).
[16]H. Zhang, D. Buchholz, and S. Passerini, "Synthesis, structure, and sodium mobility of sodium vanadium nitridophosphate: A zero-strain and safe high voltage cathode material for sodium-ion batteries," Energies **10**(7), 889 (2017).
[17]X. C. Zhang, W. Shyy, and A. M. Sastry, "Numerical simulation of intercalation-induced stress in Li-ion battery electrode particles," Journal of the Electrochemical Society **154**(10), A910–A916 (2007).
[18]Y. Li *et al.*, "Effect of local velocity on diffusion-induced stress in large-deformation electrodes of lithium-ion batteries," Journal of Power Sources **319**, 168–177 (2016).
[19]L. Brassart and Z. G. Suo, "Reactive flow in large-deformation electrodes of lithium-ion batteries," International Journal of Applied Mechanics **4**(3), 1250023 (2012).
[20]F. Q. Yang, "Comments on effects of dislocation mechanics on diffusion-induced stresses within a spherical insertion particle electrode," Journal of Materials Chemistry A **2**(40), 17183–17184 (2014).
[21]A. F. Bower, P. R. Guduru, and V. A. Sethuraman, "A finite strain model of stress, diffusion, plastic flow, and electrochemical reactions in a lithium-ion half-cell," Journal of the Mechanics and Physics of Solids **59**(4), 804–828 (2011).
[22]Z. W. Cui, F. Gao, and J. M. Qu, "A finite deformation stress-dependent chemical potential and its applications to lithium ion batteries," Journal of the Mechanics and Physics of Solids **60**(7), 1280–1295 (2012).
[23]K. J. Zhao *et al.*, "Large plastic deformation in high-capacity lithium-ion batteries caused by charge and discharge," Journal of the American Ceramic Society **94**, S226–S235 (2011).
[24]C. V. Di Leo, E. Rejovitzky, and L. Anand, "Diffusion-deformation theory for amorphous silicon anodes: The role of plastic deformation on electrochemical performance," International Journal of Solids and Structures **67-68**, 283–296 (2015).
[25]F. Q. Yang, "Effect of local solid reaction on diffusion-induced stress," Journal of Applied Physics **107**(10), 103516 (2010).
[26]Y. Li *et al.*, "Effect of local deformation on the coupling between diffusion and stress in lithium-ion battery," International Journal of Solids and Structures **87**, 81–89 (2016).
[27]K. Loeffel and L. Anand, "A chemo-thermo-mechanically coupled theory for elastic-viscoplastic deformation, diffusion, and volumetric swelling due to a chemical reaction," International Journal of Plasticity **27**(9), 1409–1431 (2011).
[28]F. Q. Yang, "Diffusion-induced bending of viscoelastic beams," International Journal of Mechanical Sciences **131**, 137–145 (2017).
[29]P. Metz, G. Alici, and G. M. Spinks, "A finite element model for bending behaviour of conducting polymer electromechanical actuators," Sensors and Actuators A: Physical **130-131**, 1–11 (2006).
[30]G. Bucci, T. Swamy, Y. M. Chiang, and W. C. Carter, "Modeling of internal mechanical failure of all-solid-state batteries during electrochemical cycling, and implications for battery design," Journal of Material Chemistry A **5**(36), 19422–19430 (2017).
[31]P. Zuo and Y. P. Zhao, "Phase field modeling of lithium diffusion, finite deformation, stress evolution and crack propagation in lithium ion battery," Extreme Mechanics Letters **9**, 467–479 (2016).